6-28-2017

Local Time Asymmetry of Saturn's Magnetosheath Flows

B. Burkholder
University of Alaska, Fairbanks

P. A. Delamere
University of Alaska, Fairbanks

X. Ma
University of Alaska, Fairbanks, max@erau.edu

M. F. Thomsen
Planetary Science Institute

R. J. Wilson
University of Colorado Boulder

See next page for additional authors

AGU PUBLICATIONS

Geophysical Research Letters

RESEARCH LETTER
10.1002/2017GL073031

Key Points:
- The magnitude of Saturn's magnetosheath plasma flow velocity in the azimuthal direction is asymmetric in local time
- The magnetopause boundary is Kelvin-Helmholtz unstable
- Implications for understanding a viscous-like interaction

Correspondence to:
P. A. Delamere,
padelamere@alaska.edu

Citation:
Burkholder, B., P. A. Delamere, X. Ma, M. F. Thomsen, R. J. Wilson, and F. Bagenal (2017), Local time asymmetry of Saturn's magnetosheath flows, *Geophys. Res. Lett.*, *44*, 5877–5883, doi:10.1002/2017GL073031.

Received 9 FEB 2017
Accepted 27 APR 2017
Accepted article online 2 MAY 2017
Published online 17 JUN 2017

Local time asymmetry of Saturn's magnetosheath flows

B. Burkholder[1], P. A. Delamere[1], X. Ma[1], M. F. Thomsen[2], R. J. Wilson[3], and F. Bagenal[3]

[1]Geophysical Institute, University of Alaska Fairbanks, Fairbanks, Alaska, USA, [2]Planetary Science Institute, Tucson, Arizona, USA, [3]Laboratory for Atmospheric and Space Physics, University of Colorado Boulder, Boulder, Colorado, USA

Abstract Using gross averages of the azimuthal component of flow in Saturn's magnetosheath, we find that flows in the prenoon sector reach a maximum value of roughly half that of the postnoon side. Corotational magnetodisc plasma creates a much larger flow shear with solar wind plasma prenoon than postnoon. Maxwell stress tensor analysis shows that momentum can be transferred out of the magnetosphere along tangential field lines if a normal component to the boundary is present, i.e., field lines which pierce the magnetopause. A Kelvin-Helmholtz unstable flow gives rise to precisely this situation, as intermittent reconnection allows the magnetic field to thread the boundary. We interpret the Kelvin-Helmholtz instability acting along the magnetopause as a tangetial drag, facilitating two-way transport of momentum through the boundary. We use reduced magnetosheath flows in the dawn sector as evidence of the importance of this interaction in Saturn's magnetosphere.

1. Introduction

The interaction of the solar wind with Saturn's rapidly rotating magnetodisc has been studied extensively from the perspective of the physical processes occurring at the magnetopause boundary [*McAndrews et al.*, 2008; *Lai et al.*, 2012; *Delamere and Bagenal*, 2013; *Delamere et al.*, 2015a; *Delamere*, 2015; *Masters et al.*, 2014; *Fuselier et al.*, 2014]. Emphasis has been placed on the influence of the solar wind on the magnetosphere. In this paper we consider the converse; namely, how does the magnetodisc interact with the magnetosheath at the solar wind-magnetosphere interface? Tangential drag at the magnetopause leads to the two-way transport of momentum, suggesting that magnetosheath flows in the prenoon sector could be significantly modified by sunward magnetospheric flows. The physical processes leading to tangential drag (often considered viscous like [*Axford and Hines*, 1961; *Axford*, 1964; *Vasyliunas*, 2015]) include, for example, the sheared-flow-driven Kelvin-Helmholtz (KH) instability and/or kinetic Alfvén waves (KAW) generated at the magnetopause boundary [*Johnson and Cheng*, 1997; *Wing et al.*, 2014]. In this paper we focus our discussion on the KH instability, following the suggestion by *Delamere and Bagenal* [2010], as means to quantify tangential drag at the magnetopause boundary. Using plasma properties (moments) derived from the Cassini Plasma Spectrometer (CAPS) data between 2004 and 2011 [*Young et al.*, 2004], we show that the flow asymmetry is indeed present with roughly a factor of 2 difference between prenoon and postnoon flows.

Desroche et al. [2013] conducted MHD simulations of solar wind flow past Saturn's polar flattened magnetosphere to understand the gross behavior of magnetosheath flows. The flattening is expected from the latitudinal confinement and radial expansion of magnetospheric plasma under the action of centrifugal stresses. Even for small flattening parameters, the equatorial tailward magnetosheath flows are reduced from those in the polar regions due to, essentially, dominant hydrodynamic flows over the poles. The asymptotic velocity found near the equatorial flanks is roughly 0.5 v_{sw}, while the polar value is roughly v_{sw}, where the subscript *sw* denotes a solar wind quantity. The interplanetary magnetic field (IMF) orientation near the magnetopause boundary is strongly influenced by the polar flattening. For an initially small angle between *y* and *z* IMF components (IMF clock angle) of +5° (−5°), the field rotates northward (southward) into the *z* (−*z*) direction as it moves toward the flanks, leading to favorable conditions for the KH instability, minimizing magnetic tension in the sheared flow direction [*Chandrasekhar*, 1961].

The presence of KH waves at Saturn's dayside magnetopause boundary has been addressed in the literature [*Masters et al.*, 2009, 2012; *Delamere et al.*, 2011; *Wilson et al.*, 2012]. In addition, *Ma et al.* [2015] demonstrated a local time asymmetry of KH waves using a two-dimensional MHD simulation with local time-dependent flow shears. Vortices forming in the prenoon and subsolar region were transported duskward by the corotating

magnetospheric flow, forming well-defined and long-lived vortex structures. We postulate that this is the reason duskside KH waves were more easily identified by *Masters et al.* [2012] and *Delamere et al.* [2011]. The growth rate of the KH instability on the dawnside is very high, and the simulations showed rapid diffusion into a boundary layer, making the identification of KH vortices difficult. Boundary normal analysis confirmed this model result with persistent boundary normal modulation by KH waves on the duskside.

It has been demonstrated that reconnection and Kelvin-Helmholtz modes interact [*Fairfield et al.*, 2000; *Otto and Fairfield*, 2000; *Hasegawa et al.*, 2004; *Ma et al.*, 2014a, 2014b]. A condition for momentum transport at the magnetopause boundary is the presence of a normal magnetic field component, producing magnetic shear stresses. Intermittent reconnection associated with the KH instability can facilitate magnetic field line threading of the magnetopause boundary. *Delamere and Bagenal* [2010] proposed the KH instability at the giant magnetospheres, driving intermittent reconnection (versus large-scale reconnection), as a plausible source of tangential drag at the magnetopause boundary. This process is analogous to the viscous-like interaction described by *Axford and Hines* [1961]. In this paper, we present evidence supporting the importance of a tangential drag at the magnetopause boundary, showing that reduced dawnside magnetosheath flows at Saturn are consistent with Maxwell stresses generated at the magnetopause boundary.

2. Data Analysis

The numerically integrated moments from CAPS (http://www.caps.lanl.gov/moments.html) through 2011 were used to calculate average flow properties in the magnetosheath [*Thomsen and Delapp*, 2005; *Thomsen et al.*, 2010]. Adequate instrument look direction is critical for determining valid moments. For simplicity we defined the magnetosheath flow directions for the dawn and dusk sectors as $-\hat{\boldsymbol{\phi}}$ and $+\hat{\boldsymbol{\phi}}$, respectively, where $\hat{\boldsymbol{\phi}}$ is the azimuthal direction. As suggested by *Thomsen et al.* [2010] we filter for points where the detector is looking into the flow, which means that in the prenoon magnetosheath we must be able to identify when the anticorotation direction is in the field of view (FOV). The CAPS moments data set available at the Planetary Data System (PDS), which is used for this study, has a flag indicating when flows in the $+\hat{\boldsymbol{\phi}}$ direction would be in the CAPS FOV. For measurements postnoon, we require that this flag is set. Since the instrument covers 2π steradian through actuation, we make the assumption that if it is not looking into the direction of corotational flow, then it is capturing anticorotational flow, so for prenoon locations we use only measurements for which the corotation flag is not set. A comparison of prenoon averages obtained using this viewing filter and averages which ignore the look direction is shown in Figure 1. As expected, selecting the correct instrument viewing always gives a set of larger values. In addition, using Saturn-centered instrument viewing [*Wilson et al.*, 2008], we also selected cases where the flow direction was fully within the instrument view and found little difference in the average V_ϕ compared to cases where the flow direction was at the edge of the instrument view, suggesting that sampling half of the distribution is sufficient for determining flow speed. These lenient restrictions are vital for obtaining meaningful statistics as the instrument is often pointed almost directly at the planet. This circumstance gives a dawnside data set which has a quarter of the data used to calculate relevant averages on the duskside and thus has half of the statistical significance quantified as standard error of the mean. In addition, data points were only selected for cases within $\pm 30°$ of latitude from the equator, and only for cases that satisfied requirements for instrument actuation and spacecraft rolling [*Thomsen et al.*, 2010].

Our expectation for a tangential drag is that the magnetosheath flows are affected by magnetospheric flows only in close proximity to the magnetopause boundary due to momentum transfer along the mostly tangential IMF field lines. Thus, we sorted our results based on time elapsed from a given boundary crossing (e.g., magnetopause and bow shock) as defined by *Delamere et al.* [2013, 2015b]. The exact locations of the boundaries following a crossing are unknown; however, we note that the Cassini spacecraft traverses approximately half of the width of the magnetosheath in 1000 min (e.g., 6 R_S at 6 km s^{-1} [*Sergis et al.*, 2013]), assuming a static magnetospheric configuration.

Using all magnetosheath values on both inbound and outbound trajectories with valid instrument viewing which occur within 500 min of a magnetopause crossing, we calculated an average azimuthal flow velocity (V_ϕ) as a function of local time. Figure 2 shows the local time variation in V_ϕ for bins with a resolution of 30 min, which shows considerable asymmetry (in magnitude and variability) relative to the subsolar point at 12 LT. We are careful to interpret the dawnward shift of the stagnation point from local noon, which is also a feature found by *Pilkington et al.* [2015], since the choice of viewing at local noon is ambiguous and we have chosen to

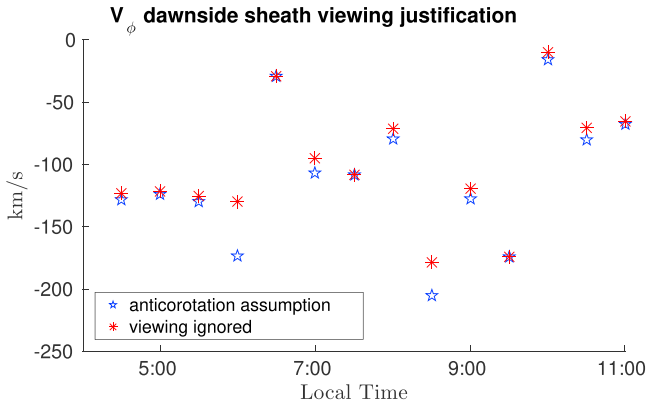

Figure 1. Comparison of dawnside V_ϕ averages in local time obtained by selecting "noncorotating" instrument viewing (blue) versus the same calculation where the look direction is not considered (red). The average percentage difference across all bins is calculated as 10%.

filter for positively directed azimuthal flow in this region. The blue-shaded bars give an average of the prenoon or postnoon values, excluding those at [11:30, 12:00] and [12:00, 12:30] in lieu of ambiguous viewing. For the remainder of this paper we will use an estimate of 125 km s^{-1} for the dawnside and 200 km s^{-1} for the duskside as representative values for the average V_ϕ.

Figure 3 (left column) shows the dependence on spacecraft time from the magnetopause boundary crossing of the average flows in the local time sectors 7:00–11:00 and 13:00–17:00. It is clear that the dawnside flow speed (red) is lower than the duskside (blue) by ~75-100 km s^{-1}, and this deficit gradually lessens as Cassini's presumed distance to the magnetopause boundary increases. A calculation of distance from the boundary cannot be made with the spacecraft time and its velocity since the magnetopause may be moving in response to solar wind conditions at a rate which we cannot determine. However, the time elapsed from the boundary over which the deficit exists suggests that a significant fraction of magnetosheath flows are reduced from the expected asymptotic value of 200 km s^{-1} [*Desroche et al.*, 2013]. The spread of values indicated by the percentile bars is clearly larger on the dawnside, which may not be strictly due to asymmetric local time sampling of the spacecraft, but has physical significance in terms of variability in flow conditions. Additionally, Figure 3 (right column) shows the time elapsed from bow shock crossings into the magnetosheath where time now

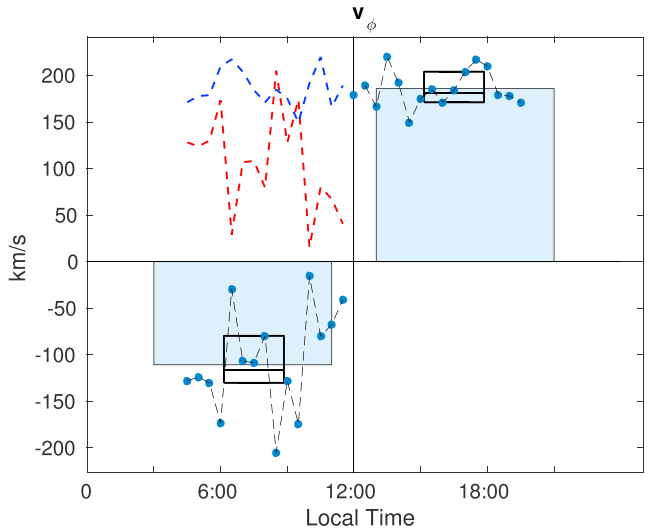

Figure 2. Saturn's average V_ϕ magnetosheath flows in 30 min local time bins. The blue bars show the dawn versus dusk average, excluding 11:30 to 12:30, while the box plot (black) gives the 25th, 50th, and 75th percentiles of the points included in this average. The blue dashed line is the mirror of the dusk velocities across the *y* axis, while the red is the dawn velocities mirrored across the *x* axis.

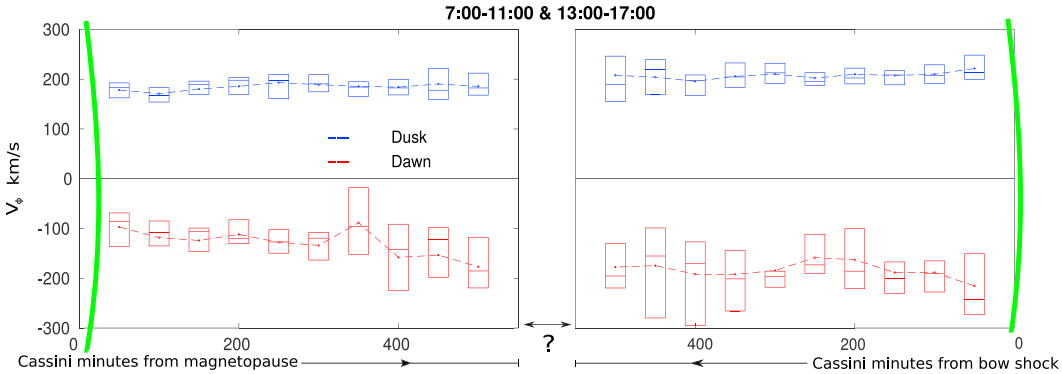

Figure 3. The first 500 min after each (left column) magnetopause or (right column) bow shock boundary crossing. The value of each point above is calculated as an average of the relevant time bin across all boundary crossings in the corresponding prenoon or postnoon sectors given in the title. The error bars give the 25th, 50th, and 75th percentiles of the data used to calculate the average. Green curves represent the boundaries, and the question mark portrays that we are always unsure as to the actual distance to either boundary.

increases from right to left. The apparent dawn-dusk symmetry for flows in proximity to the bow shock shows that the flow deficit exists for only the magnetosheath nearest to the magnetopause.

3. Discussion

Our interpretation of the dawn-dusk asymmetry of Saturn's magnetosheath flows is summarized in Figure 4. The region of reduced flow is illustrated by the shaded region (red), showing a gradient in flow deficit as a function of proximity to the magnetopause boundary. The Kelvin-Helmholtz vortices (green) highlight the dawn-dusk asymmetry modeled by *Ma et al.* [2015], whereby vortices observed in the dusk sector were formed in the subsolar region and advected duskward by corotational flows in the magnetosphere. Postnoon, the flow shear is minimized and thus the KH waves no longer actively grow. The highly KH unstable dawnside boundary, on the other hand, can mediate momentum transfer.

Intermittent reconnection associated with KH could play an important role in quantifying the role of a viscous-like interaction; therefore, we use this concept as a starting point to discuss the dawnside momentum transfer. An estimate of the momentum transfer process can be made by considering the flux conservative form of the momentum equation in steady state which is given by *Vasyliunas* [2015], i.e.,

$$\nabla \cdot \left[\rho \mathbf{uu} + \mathbf{P} + \frac{B^2}{2\mu_o}\mathbf{I} - \frac{\mathbf{BB}}{\mu_o}\right] = 0 \tag{1}$$

If we assume that the momentum flux density of the magnetosheath flow is conserved in the absence of momentum transfer from the magnetosphere, then $\nabla \cdot \rho \mathbf{uu} = 0$. For tangential momentum transfer normal to the boundary surface and the assumption of isotropic pressure, only the first and last terms of the steady state momentum equation can represent shear stresses through off diagonal elements. Let $+\hat{\mathbf{t}}$ be the tangential magnetosheath flow (tailward) direction and $+\hat{\mathbf{n}}$ be the direction normal to the magnetopause boundary, pointing from the magnetosphere to the magnetosheath. If the magnetosheath flow is modified (i.e., reduced) due to Maxwell shear stresses at the magnetopause boundary, then $\mathbf{BB} \approx -B_t B_n \hat{\mathbf{t}}\hat{\mathbf{n}}$ (blue lines in Figure 4). Indeed, we can also consider the Reynolds stress, $(\rho u_t u_n)\hat{\mathbf{t}}\hat{\mathbf{n}}$; however, since the momentum flux due to Maxwell stresses is 2–3 times larger [*Miura*, 1984], we omit this contribution from our calculations.

The momentum transfer from the solar wind to the magnetosphere was investigated by *Delamere and Bagenal* [2013] in terms of the limiting case where the IMF fully threads the magnetopause boundary. In this limit, the giant magnetospheres can essentially be treated as a comet-like interaction where the solar wind is mass loaded by the magnetospheric plasma sources. Following the Walén relation for an Alfvénic interaction, the maximum momentum flux density delivered to the magnetosphere is

$$\frac{\mathbf{BB}}{\mu_o} \approx \frac{M_{sw} B_{IMF}^2}{\mu_o}\hat{\mathbf{t}}\hat{\mathbf{n}} \tag{2}$$

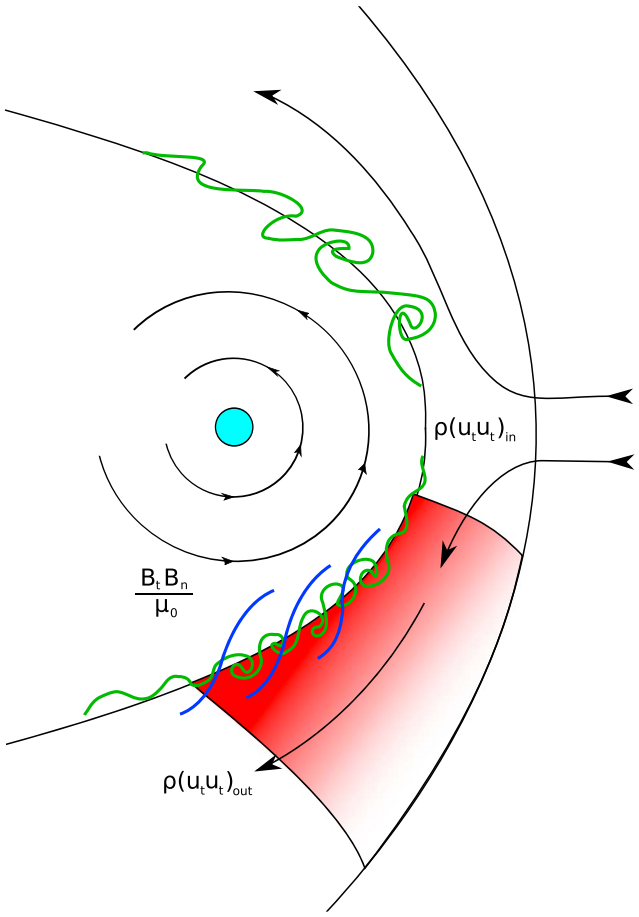

Figure 4. Magnetic field lines (blue) thread the dawnside magnetopause boundary in the presence of Kelvin-Helmholtz waves (green). The tangential and normal components of the magnetic field across the magnetopause boundary constitute Maxwell shear stresses, facilitating momentum transfer. The shaded area shows a gradient representing the severity of the momentum deficit.

where M_{sw} is the solar wind Mach number and B_{IMF} is the IMF strength. The volume integral of the steady momentum equation can be written as a surface integral via the divergence theorem, or

$$\int (\rho u_t u_t)_{sh} da_t = \int \frac{B_t B_n}{\mu_o} da_n \tag{3}$$

where the subscript "sh" refers to magnetosheath quantities and where da_t refers to the magnetosheath inflow/outflow surfaces and da_n is the magnetopause boundary. The ratio of tangential area to the normal area is estimated to be $a_t/a_n \sim 1/5$ for an affected magnetosheath width $\sim 3\ R_S$ and a distance along the magnetopause boundary from 7 to 10 LT $\sim 15\ R_S$. This area ratio estimate avoids the flank/tail region where flows may not be corotational and is based on the effected magnetosheath width from the data (Figure 3). The average magnetosheath number density in this region from the numerical moments is 0.18 cm^{-3}. If we assume that the interplanetary magnetic field, on average, is 0.5 nT [*Jackman and Arridge*, 2011] and use the flow deficit from the expected value calculated from the data $(\Delta u_t)_{sh} \sim 75$ km s^{-1}, then we find

$$\rho (\Delta u_t)^2_{sh} \left(\frac{\mu_o}{M_{sw} B^2_{IMF}} \right) \left(\frac{a_t}{a_n} \right) \sim 0.2 \tag{4}$$

Thus, the momentum flux deficit is consistent with the solar wind transferring a significant fraction of the maximum possible momentum to the magnetosphere in the dayside sector. The fully draped IMF field configuration is not expected to be realized until farther downstream in the tail region, yet the momentum transfer is found to be substantial.

Alternatively, we could consider preferential mass transport from the magnetosphere, leading to a net mass loading of the magnetosheath. In the case of KH, the $\rho u_t u_n$ term in equation (1) would be unbalanced, with more momentum flux directed from the magnetosphere to the magnetosheath. For a diffusive transport process like KAW, the effective mass loading of the sheath could be treated with a mass loading term on the right-hand side of equation (1), such that $\rho(\Delta u^2)_{sh} a_t = \dot{M} u_{ms}$, where $\dot{M}$ is the net mass loading rate of the sheath and u_{ms} is the magnetospheric flow speed (upper limit) in the Saturn/Sun reference frame. For $u_{ms} = 100$ km s^{-1} and $a_t = 3{\times}4\ R_S^2$, $\dot{M} \sim 1$ kg s^{-1}. This is a small fraction of the plasma mass transport rates of 50–100 kg s^{-1} from Enceladus [*Fleshman et al.*, 2013].

Finally, we conclude that our findings are consistent with the 7% dawnward shift of the magnetopause boundary discussed by *Pilkington et al.* [2015], who also attributed their finding to "the intrinsic asymmetry in plasma flow around the planet with respect to the direction of solar wind flow." Although the solar wind is the primary driver of the system, magnetospheric phenomena could also contribute to the dynamics of the plasma flow. In simulations by *Kivelson and Jia* [2014], a system of field-aligned currents rotating with the planet produces modulations in field and plasma conditions which occur at the planetary oscillation period. The asymmetry in the shape of the magnetopause which they found in simulations was similar, albeit larger, than that found from the data study by *Pilkington et al.* [2015], suggesting that internal drivers could also influence dawn/dusk asymmetry. Fundamentally, however, the solar wind interaction must be at the root of observed dawn/dusk asymmetries.

4. Conclusions

We summarize our findings as follows.

1. Cassini plasma data show an asymmetry of ~75 km s^{-1} between the dawnside and duskside of Saturn's magnetosheath. We interpret this as a consequence of the flow shear between the solar wind and corotational magnetosphere plasma which is maximized on the prenoon flank.
2. Saturn's interaction with the solar wind could be dominated by viscous-like processes at the magnetopause boundary — a situation that is very different from Earth where large-scale Dungey reconnection dominates.
3. The momentum deficit in Saturn's dawnside magnetosheath is consistent with maximum momentum transfer via magnetic shear stresses from the solar wind.
4. The large momentum transfer to the magnetosphere suggests that local time asymmetries in magnetospheric dynamics are strongly influenced by the solar wind interaction.
5. The dawn flank is subject to significant flow shears and is likely subject to ongoing Kelvin-Helmholtz instability and related intermittent and small-scale reconnection.
6. Similar considerations are applicable to any giant magnetosphere whose corotating magnetodisc creates a sheared flow with the solar wind which is asymmetric in local time, i.e., Jupiter. The hydrodynamic conditions of this configuration imply an asymmetry of the type we present here.

Acknowledgments
The authors acknowledge support from NASA grant NNX11AK80G. Work at PSI was supported by the NASA Cassini Project through JPL contract 1243218 with Southwest Research Institute. CAPS/IMS ion moments are available as a pre-peer-reviewed data product at the PDS (http://ppi.pds.nasa.gov/search/view/?f=yes&id=pds://PPI/CO-S_SW-CAPS-5-DDR-ION-MOMENTS-V1.0)

References

Axford, W. I. (1964), Viscous interaction between the solar wind and the Earth's magnetosphere, *Planet. Space Sci.*, *12*, 45–53.
Axford, W. I., and C. O. Hines (1961), A unifying theory of high latitude geophysical phenomena and geomagnetic storms, *Can. J. Phys.*, *39*, 1433–1464.
Chandrasekhar, S. (1961), *Hydrodynamic and Hydromagnetic Stability*, International Series of Monographs on Physics, Clarendon, Oxford.
Delamere, P. A. (2015), *Magnetotails in the Solar System*, chap. Solar Wind Interaction With the Giant Magnetospheres and Earth's Magnetosphere, John Wiley, Hoboken, N. J.
Delamere, P. A., and F. Bagenal (2010), Solar wind interaction with Jupiter's magnetosphere, *J. Geophys. Res.*, *115*, A10201, doi:10.1029/2010JA015347.
Delamere, P. A., and F. Bagenal (2013), Magnetotail structure of the giant magnetospheres: Implications of the viscous interaction with the solar wind, *J. Geophys. Res. Space Physics*, *118*, 7045–7053, doi:10.1002/2013JA019179.
Delamere, P. A., R. J. Wilson, and A. Masters (2011), Kelvin-Helmholtz instability at Saturn's magnetopause: Hybrid simulations, *J. Geophys. Res.*, *116*, A10222, doi:10.1029/2011JA016724.
Delamere, P. A., R. J. Wilson, S. Eriksson, and F. Bagenal (2013), Magnetic signatures of Kelvin-Helmholtz vortices on Saturn's magnetopause: Global survey, *J. Geophys. Res. Space Physics*, *118*, 393–404, doi:10.1029/2012JA018197.
Delamere, P. A., F. Bagenal, C. Paranicas, A. Masters, A. Radioti, B. Bonfond, L. Ray, X. Jia, J. Nichols, and C. Arridge (2015a), Solar wind and internally driven dynamics: Influences on magnetodiscs and auroral responses, *Space Sci. Rev.*, *187*, 51–97, doi:10.1007/s11214-014-0075-1.
Delamere, P. A., A. Otto, X. Ma, F. Bagenal, and R. J. Wilson (2015b), Magnetic flux circulation in the rotationally driven giant magnetospheres, *J. Geophys. Res. Space Physics*, *120*, 4229–4245, doi:10.1002/2015JA021036.
Desroche, M., F. Bagenal, P. A. Delamere, and N. Erkaev (2013), Conditions at the magnetopause of Saturn and implications for the solar wind interaction, *J. Geophys. Res. Space Physics*, *118*, 3087–3095, doi:10.1002/jgra.50294.

Fairfield, D. H., A. Otto, T. Mukai, S. Kokubun, R. P. Lepping, J. T. Steinberg, A. J. Lazarus, and T. Yamamoto (2000), Geotail observations of the Kelvin-Helmholtz instability at the equatorial magnetotail boundary for parallel northward fields, *J. Geophys. Res.*, *105*, 21,159–21,174, doi:10.1029/1999JA000316.

Fleshman, B. L., P. A. Delamere, F. Bagenal, and T. Cassidy (2013), A 1-D model of physical chemistry in Saturn's inner magnetosphere, *J. Geophys. Res. Planets*, *118*, 1567–1581, doi:10.1002/jgre.20106.

Fuselier, S. A., R. Frahm, W. S. Lewis, A. Masters, J. Mukherjee, S. M. Petrinec, and I. J. Sillanpaa (2014), The location of magnetic reconnection at Saturn's magnetopause: A comparison with Earth, *J. Geophys. Res. Space Physics*, *119*, 2563–2578, doi:10.1002/2013JA019684.

Hasegawa, H., M. Fujimoto, T. Phan, H. Reme, A. Balogh, M. Dunlop, C. Hashimoto, and R. TanDokoro (2004), Transport of solar wind into Earth's magnetosphere through rolled-up Kelvin-Helmholtz vortices, *Nature*, *430*, 755–758, doi:10.1038/nature02799.

Jackman, C. M., and C. S. Arridge (2011), Solar cycle effects on the dynamics of Jupiter's and Saturn's magnetospheres, *Sol. Phys.*, *274*, 481–502, doi:10.1007/s11207-011-9748-z.

Johnson, J. R., and C. Z. Cheng (1997), Kinetic Alfvén waves and plasma transport at the magnetopause, *Geophys. Res. Let*, *24*, 1423–1426, doi:10.1029/97GL01333.

Kivelson, M. G., and X. Jia (2014), Control of periodic variations in Saturn's magnetosphere by compressional waves, *J. Geophys. Res. Space Physics*, *119*, 8030–8045, doi:10.1002/2014JA020258.

Lai, H. R., H. Y. W. C. T. Russell, C. S. Arridge, and M. K. M. K. Dougherty (2012), Reconnection at the magnetopause of Saturn: Perspective from FTE occurrence and magnetosphere size, *J. Geophys. Res.*, *117*, A05222, doi:10.1029/2011JA017263.

Ma, X., A. Otto, and P. A. Delamere (2014a), Interaction of magnetic reconnection and Kelvin-Helmholtz modes for large magnetic shear: 1. Kelvin-Helmholtz trigger, *J. Geophys. Res. Space Physics*, *119*, 781–797, doi:10.1002/2013JA019224.

Ma, X., A. Otto, and P. A. Delamere (2014b), Interaction of magnetic reconnection and Kelvin-Helmholtz modes for large magnetic shear: 2. Reconnection trigger, *J. Geophys. Res. Space Physics*, *119*, 808–820, doi:10.1002/2013JA019225.

Ma, X., B. Stauffer, P. A. Delamere, and A. Otto (2015), Asymmetric Kelvin-Helmholtz propagation at Saturn's dayside magnetopause, *J. Geophys. Res. Space Physics*, *120*, 1867–1875, doi:10.1002/2014JA020746.

Masters, A., N. Achilleos, C. Bertucci, M. K. Dougherty, S. J. Kanani, C. S. Arridge, H. J. McAndrews, and A. J. Coates (2009), Surface waves on Saturn's dawn flank magnetopause driven by the Kelvin-Helmholtz instability, *Planet. Space Sci.*, *57*, 1769–1778, doi:10.1016/j.pss.2009.02.010.

Masters, A., N. Achilleos, J. C. Cutler, A. J. Coates, M. K. Dougherty, and G. H. Jones (2012), Surface waves on Saturn's magnetopause, *Planet. Space Sci.*, *65*, 109–121, doi:10.1016/j.pss.2012.02.007.

Masters, A., M. Fujimoto, H. Hasegawa, C. T. Russell, A. J. Coates, and M. K. Dougherty (2014), Can magnetopause reconnection drive Saturn's magnetosphere?, *Geophys. Res. Let*, *41*, 1862–1868, doi:10.1002/2014GL059288.

McAndrews, H. J., C. J. Owen, M. F. Thomsen, B. Lavraud, A. J. Coates, M. K. Dougherty, and D. T. Young (2008), Evidence for reconnection at Saturn's magnetopause, *J. Geophys. Res.*, *113*, A04210, doi:10.1029/2007JA012581.

Miura, A. (1984), Anomalous transport by magnetohydrodynamic Kelvin-Helmholtz instabilities in the solar wind-magnetosphere interaction, *J. Geophys. Res.*, *89*, 801–818, doi:10.1029/JA089iA02p00801.

Otto, A., and D. H. Fairfield (2000), Kelvin-Helmholtz instability at the magnetotail boundary: MHD simulation and comparison with Geotail observations, *J. Geophys. Res.*, *105*, 21,175–21,190, doi:10.1029/1999JA000312.

Pilkington, N. M., N. Achilleos, C. S. Arridge, P. Guio, A. Masters, L. C. Ray, N. Sergis, M. F. Thomsen, A. J. Coates, and M. K. Dougherty (2015), Asymmetries observed in Saturn's magnetopause geometry, *Geophys. Res. Let*, *42*, 6890–6898, doi:10.1002/2015GL065477.

Sergis, N., C. M. Jackman, A. Masters, S. M. Krimigis, M. F. Thomsen, D. C. Hamilton, D. G. Mitchell, M. K. Dougherty, and A. J. Coates (2013), Particle and magnetic field properties of the Saturnian magnetosheath: Presence and upstream escape of hot magnetospheric plasma, *J. Geophys. Res. Space Physics*, *118*, 1620–1634, doi:10.1002/jgra.50164.

Thomsen, M. F., and D. M. Delapp (2005), Numerical moments computation for CAPS/IMS, *Tech. Rep. LA-UR-05-1542*, Los Alamos Natl. Lab., Los Alamos, N. M.

Thomsen, M. F., D. B. Reisenfeld, D. M. Delapp, R. L. Tokar, D. T. Young, F. J. Crary, E. C. Sittler, M. A. McGraw, and J. D. Williams (2010), Survey of ion plasma parameters in Saturn's magnetosphere, *J. Geophys. Res.*, *115*, A10220, doi:10.1029/2010JA015267.

Vasyliunas, V. M. (2015), *Magnetotail: Unsolved Fundamental Problem of Magnetospheric Physics*, pp. 1–19, John Wiley, Hoboken, N. J., doi:10.1002/9781118842324.ch1.

Wilson, R. J., R. L. Tokar, M. G. Henderson, T. W. Hill, M. F. Thomsen, and D. H. Pontius (2008), Cassini plasma spectrometer thermal ion measurements in Saturn's inner magnetosphere, *J. Geophys. Res.*, *113*, A12218, doi:10.1029/2008JA013486.

Wilson, R. J., P. A. Delamere, F. Bagenal, and A. Masters (2012), Kelvin-Helmholtz instability at Saturn's magnetopause: Cassini ion data analysis, *J. Geophys. Res.*, *117*, A03212, doi:10.1029/2011JA016723.

Wing, S., J. R. Johnson, C. C. Chaston, M. Echim, C. P. Escoubet, B. Lavraud, C. Lemon, K. Nykyri, A. Otto, J. Raeder, and C.-P. Wang (2014), Review of solar wind entry into and transport within the plasma sheet, *Space Sci. Rev.*, *184*(1), 33–86, doi:10.1007/s11214-014-0108-9.

Young, D. T., et al. (2004), Cassini plasma spectrometer investigation, *Space Sci. Rev.*, *114*, 1–4, doi:10.1007/s11214-004-1406-4.